

# Comparison of Protective Effects against Reactive Oxygen Species of Mononuclear and Dinuclear Cu(II) Complexes with *N*-Substituted Benzothiazolesulfonamides

Marta González-Álvarez,<sup>†</sup> Gloria Alzuet,<sup>†</sup> Joaquín Borrás,<sup>\*,†</sup> Lucas del Castillo Agudo,<sup>‡</sup> Santiago García-Granda,<sup>§</sup> and José Manuel Montejo-Bernardo<sup>§</sup>

*Departamento de Química Inorgánica and Departamento de Microbiología y Ecología, Facultad de Farmacia, Universitat de València, Avda. Vicent Andrés Estellés s/n, 46100 Burjassot, Spain, and Departamento de Química-Física y Analítica, Universidad de Oviedo, Avda. Julián Clavería 8, 33006 Oviedo, Spain*

Received January 24, 2005

Copper(II) complexes of *N*-benzothiazolesulfonamides (HL<sup>1</sup> = *N*-2-(4-methylphenylsulfamoyl)-6-nitro-benzothiazole, HL<sup>2</sup> = *N*-2-(phenylsulfamoyl)-6-chloro-benzothiazole, and HL<sup>3</sup> = *N*-2-(4-methylphenylsulfamoyl)-6-chloro-benzothiazole) with ammonia have been synthesized and characterized. The crystal structures of the [Cu(L<sup>1</sup>)<sub>2</sub>(NH<sub>3</sub>)<sub>2</sub>]·2MeOH (**1**), [Cu(L<sup>2</sup>)<sub>2</sub>(NH<sub>3</sub>)<sub>2</sub>] (**2**), and [Cu(L<sup>3</sup>)<sub>2</sub>(NH<sub>3</sub>)<sub>2</sub>] (**3**) compounds have been determined. Compounds **1** and **2** present a distorted square planar geometry. In both compounds the metal ion is coordinated by two benzothiazole N atoms from two sulfonamidate anions and two NH<sub>3</sub> molecules. Complex **3** is distorted square-pyramidal. The Cu(II) ion is linked to the benzothiazole N and sulfonamidate O atoms of one of the ligands, the benzothiazole N of another sulfonamidate anion, and two ammonia N atoms. We have tested the superoxide dismutase (SOD)-like activity of the compounds and compared it with that of two dinuclear compounds [Cu<sub>2</sub>(L<sup>4</sup>)<sub>2</sub>(OCH<sub>3</sub>)<sub>2</sub>(NH<sub>3</sub>)<sub>2</sub>] (**4**) and [Cu<sub>2</sub>(L<sup>4</sup>)<sub>2</sub>(OCH<sub>3</sub>)<sub>2</sub>(dmsO)<sub>2</sub>] (**5**) (HL<sup>4</sup> = *N*-2-(phenylsulfamoyl)-4-methyl-benzothiazole). In vitro indirect assays show that the dimeric complexes are better SOD mimics than the monomeric ones. We have also assayed the protective action provided by the compounds against reactive oxygen species over Δ*sod1* mutant of *Saccharomyces cerevisiae*. In contrast to the in vitro results, the mononuclear compounds were more protective to SOD-deficient *S. cerevisiae* strains than the dinuclear complexes.

## 1. Introduction

Free radicals represent one of the main causes of both cellular damage and numerous degenerative diseases.<sup>1,2</sup> A predominant cellular free radical is an oxygen-derived species, superoxide anion (O<sub>2</sub><sup>•−</sup>), that is formed by the leakage of high-energy electrons along mitochondrial electron transport chains and by a variety of cytosolic and membrane-bound enzymes, including xanthine oxidase and cytochrome P450 complexes.<sup>3</sup> O<sub>2</sub><sup>•−</sup> mediates direct cell damage and

reacts with hydrogen peroxide (H<sub>2</sub>O<sub>2</sub>) and nitric oxide radicals to generate the extremely reactive species hydroxyl radical (HO<sup>•</sup>) and peroxynitrite (ONOO<sup>−</sup>), respectively.<sup>4</sup> The first line of cellular defense is the superoxide dismutases (SODs), the metalloenzymes which catalyze the dismutation of superoxide anions into hydrogen peroxide and dioxygen. Increasing intracellular levels of SOD or administering exogenous SOD has been investigated for use in protection against oxidative injury, but the results were disappointing because, as a protein, SOD has a number of delivery and stability shortcomings.<sup>5</sup> To circumvent such limitations, there is considerable interest in developing synthetic SOD mimics that have low molecular weight, biological stability, mem-

\* E-mail: Joaquin.Borras@uv.es. Telephone: 00 34 963544530. Fax: 00 34 963544960.

<sup>†</sup> Departamento de Química Inorgánica, Universitat de València.

<sup>‡</sup> Departamento de Microbiología y Ecología, Universitat de València.

<sup>§</sup> Departamento de Química-Física y Analítica, Universidad de Oviedo.

(1) Halliwell, B.; Gutteridge, J. M. C. *Free Radicals in Biology and Medicine*, 3rd ed.; Oxford University: New York, 1999.

(2) Simonian, N. A.; Coyle, J. T. *Annu. Rev. Pharmacol. Toxicol.* **1996**, *36*, 83.

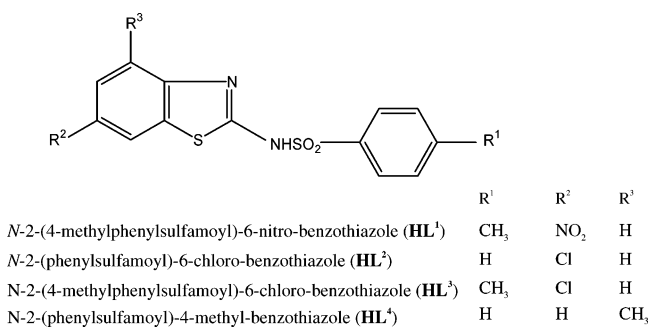
(3) Fridovich, I. *Annu. Rev. Pharmacol. Toxicol.* **1993**, *23*, 239.

(4) Beckman, J. S.; Koppenol, W. H. *Am. J. Physiol.* **1996**, *271C*, 424.

(5) Weiss, R. H.; Riley, D. P. *Therapeutic Aspects of Manganese(II)-based Superoxide Dismutase Mimics*. In *Uses of Inorganic chemistry in Medicine*; Farrell N. P., Ed; Royal Society of Chemistry: Cambridge, 1999.

brane permeability, nontoxicity, and cost-effectiveness.<sup>6</sup> The search for SOD mimics yielded a variety of chelates of transition metals such as copper.<sup>7–9</sup> In this study, we have published several papers describing the SOD mimic activity of copper complexes with *N*-substituted sulfonamides.<sup>10–15</sup> Other pharmacological properties have been reported in detail for a large number of metal complexes of sulfonamides.<sup>16</sup>

Numerous indirect assays, such as the nitro blue tetrazolium (NBT) or cytochrome *c* or brazilin assays, have been used in attempts to measure the SOD activity of putative SOD mimics.<sup>17–21</sup> However these assays, which typically rely on a spectrophotometric change of a redox indicator to measure superoxide levels, cannot kinetically distinguish between a catalytic dismutation of superoxide and a stoichiometric interaction of superoxide with the putative SOD mimic. The direct methods to determine the SOD activity, pulse radiolysis, and stopped-flow kinetic analysis help elucidate if the complexes are a true catalyst or not, but the concentration of superoxide anions is higher than that observed in vivo. In fact, several SOD mimics which showed very efficient SOD-like activity in vitro failed to do so in vivo.<sup>22–25</sup> Thus far, none of the assays currently employed can exactly replicate the environment encountered by these SOD mimics in the cellular moiety. As a consequence we have proposed a new method based on the protection of the complexes against oxidative stress over three different strains of *Saccharomyces cerevisiae*.<sup>11</sup>

Scheme 1. *N*-Substituted Sulfonamides

As a continuation of our research, we describe the synthesis, structural determination, and spectroscopic properties of three mononuclear copper complexes with *N*-substituted sulfonamides (Scheme 1). A study of the SOD mimetic activity in vitro and the protection against reactive oxygen species in vivo of these compounds and two dinuclear complexes previously synthesized<sup>26</sup> is reported.

## 2. Experimental Section

**Materials and Methods.** Reagents and solvents were commercially available and were used without further purification. Elemental analyses (C, N, H, S) were performed on a Carlo Erba AAS instrument. IR spectra (KBr disks) were obtained using a Mattson Satellite FT-IR in the range 4000–400 cm<sup>–1</sup>. Fast atomic bombardment (FAB) mass spectra were obtained on a VG Autospec spectrometer with 3-nitrobenzyl alcohol as a matrix. The electrospray mass spectra, in positive mode (ESI<sup>+</sup>), of the compounds dissolved in dmso:EtOH [1:4] were obtained from an ESQUIRE 3000 Plus (Bruker) ion trap mass spectrometer. Diffuse reflectance spectra (Nujol mulls) of the complexes were recorded on a Shimadzu UV-2101 PC spectrophotometer. Electronic paramagnetic resonance (EPR) spectra obtained at the X-band frequency at room temperature with a Bruker ELEXSYS spectrometer.

**Synthesis of the Ligands.** *N*-2-(4-Methylphenylsulfamoyl)-6-nitro-benzothiazole (**HL**<sup>1</sup>). A mixture containing 1 g of 2-amino-6-nitrobenzothiazole and 2.5 g of toluene-4-sulfonyl chloride in 6 mL of pyridine was heated at reflux for 1 h. Then, it was added to 10 mL of cold water and stirred for several minutes. A solid was obtained and it was purified using ethanol.<sup>27</sup> Data for compound *N*-2-(4-sulfamoyl)-6-nitro-benzothiazole (**HL**<sup>1</sup>) (1.786 g, 74%) found: C, 56.75; H, 2.96; N, 12.03; S, 17.11. C<sub>14</sub>H<sub>11</sub>N<sub>3</sub>S<sub>2</sub>O<sub>2</sub>Cl requires C, 56.93; H, 3.14; N, 12.04; S, 16.32, M 349.  $\bar{\nu}_{\text{max}}$ /cm<sup>–1</sup>: 1550 (thiazole); 1314, 1151 (SO<sub>2</sub>); 955 (S–N). FAB:  $m/z$  350 (M<sup>+</sup>). Solid UV–vis ( $\lambda_{\text{max}}$ /nm): 371, 509(sh).

*N*-2-(Phenylsulfamoyl)-6-chloro-benzothiazole (**HL**<sup>2</sup>) and *N*-2-(4-Methylphenylsulfamoyl)-6-chloro-benzothiazole (**HL**<sup>3</sup>). These ligands were obtained and characterized as previously reported.<sup>10,12</sup>

**Synthesis of the Complexes.** [Cu(L<sup>1</sup>)<sub>2</sub>(NH<sub>3</sub>)<sub>2</sub>]·2MeOH (**1**), [Cu(L<sup>2</sup>)<sub>2</sub>(NH<sub>3</sub>)<sub>2</sub>] (**2**), and [Cu(L<sup>3</sup>)<sub>2</sub>(NH<sub>3</sub>)<sub>2</sub>] (**3**). We dissolved 1 mmol of the corresponding benzothiazolesulfonamide in 30 mL of methanol plus 2 mL of aqueous NH<sub>3</sub> (30%). This solution was added dropwise to 20 mL of a methanolic solution containing 1 mmol of Cu(NO<sub>3</sub>)<sub>2</sub>·3H<sub>2</sub>O. The resulting mixture was stirred for several hours. A violet solid was formed and removed by filtration. After a few days, black crystals for **1** and **3** and violet crystals for **2** were obtained from the filtrate after slow evaporation at room

- (6) Dowling, E. J.; Chander, C. L.; Claxson, A. W.; Lillie, C.; Blake, D. R. *Free Radical Res. Commun.* **1993**, *18*, 291.
- (7) Müller, J.; Felix, K.; Maichle, C.; Lengfelder, E.; Strahle, I.; Weser, U. *Inorg. Chim. Acta* **1994**, *47*, 853.
- (8) Pierre, J. L.; Chautemps, P.; Refaif, S.; Beguin, C.; Marzouki, A. E.; Serratricel, G. *J. Am. Chem. Soc.* **1995**, *117*, 1965.
- (9) Batinić-Haberle, I.; Spasojević, I.; Stevens, R. D.; Hambright, P.; Pedatsur, N.; Okado-Matsumoto, A.; Fridovich, I. *Dalton Trans.* **2004**, 1696.
- (10) González-Álvarez, M.; Alzuet, G.; Borrás, J.; Macías, B.; Montejo, J. M.; García-Granda, S. *Z. Anorg. Allg. Chem.* **2003**, *629*, 112.
- (11) González-Álvarez, M.; Alzuet, G.; Borrás, J.; del Castillo-Agudo, L.; Montejo-Bernardo, J. M.; García-Granda, S. *J. Biol. Inorg. Chem.* **2003**, *8*, 112.
- (12) González-Álvarez, M.; Alzuet, G.; Borrás, J.; del Castillo, L.; García-Granda, S.; Montejo, J. M. *J. Inorg. Biochem.* **2004**, *98*, 189.
- (13) Casanova, J.; Alzuet, G.; Borrás, J.; LaTorre, J.; Sanau, M.; García-Granda, S. *J. Inorg. Biochem.* **1995**, *60*, 219.
- (14) Casanova, J.; Alzuet, G.; Borrás, J.; Carugo, O. *J. Chem. Soc., Dalton Trans.* **1996**, 2239.
- (15) Casanova, J.; Alzuet, G.; Borrás, J.; Ferrer, S.; LaTorre, J. A.; Ramírez, J. *Inorg. Chim. Acta* **2000**, *304*, 170.
- (16) Borrás, J.; Alzuet, G.; Ferrer, S.; Supuran, C. T. In *Metal complexes of heterocyclic Sulfonamides as Carbonic Anhydrase Inhibitors in Carbonic Anhydrase. Its Inhibitors and Activators*; Supuran, C. T., Scozzafava, A., Conway, J., Eds.; CRC Press: Boca Raton, 2004.
- (17) Beauchamp, C.; Fridovich, I. *Anal. Biochem.* **1971**, *44*, 276.
- (18) Lienhard, G. E.; Slot, J. W.; James, D. E.; Mueckler, M. M. *Sci. Am.* **1992**, *267*, 86.
- (19) Kahn, C. R.; White, M. F. *J. Clin. Invest.* **1988**, *82*, 1151.
- (20) White, M. F.; Shaleson, S. E.; Keutmann, H.; Kahn, C. R. *J. Biol. Chem.* **1988**, *263*, 2969.
- (21) Fisher, A. E. O.; Maxwell, S. C.; Naughton, D. P. *Inorg. Chem. Commun.* **2003**, *6*, 1205.
- (22) Riley, D. P.; Rivers, W. J.; Weiss, R. H. *Anal. Biochem.* **1991**, *196*, 344.
- (23) Riley, D. P. *Chem. Rev.* **1999**, *99*, 2573.
- (24) Goldstein, S.; Czapski, G. *Free Radical Res. Commun.* **1991**, *12*, 13.
- (25) Aranovitch, J.; Samuni, A.; Godinger, A.; Czapski, G. In *Superoxide and superoxide dismutase in chemistry, biology and medicine*; Rotilio G., Ed.; Elsevier Science Publishers: New York, 1986.

- (26) González-Álvarez, M.; Alzuet, G.; Borrás, J.; García-Granda, S.; Montejo, J. M. *J. Inorg. Biochem.* **2003**, *96*, 443.
- (27) Vogel, A. I. *Longman Scientific & Technical*, 1989.

temperature. Crystals of **1**, **2**, and **3** were isolated by filtration, washed with methanol, and dried under vacuum.

Complex **1** (0.282 g, 65.8%) found: C, 41.72; N, 13.10; H, 4.00; S, 15.02.  $C_{30}H_{34}CuN_8O_{10}S_4$  requires C, 41.97; N, 13.06; H, 3.99; S, 14.94.  $\nu_{\max}/\text{cm}^{-1}$ : 1455 (thiazole); 1284, 1143–1126 ( $\text{SO}_2$ ); 973 (S–N). Solid UV–vis ( $\lambda_{\max}/\text{nm}$ ): 600. ESI-MS gives a peak at  $m/z = 858$ . Conductivity measurements in dmsO:EtOH (1:4) solutions: 34.5  $\mu\text{S}/\text{cm}$ .

Complex **2** (0.178 g, 47.9%) found: C, 41.91; N, 11.30; H, 2.99; S, 17.41.  $C_{26}H_{22}Cl_2CuN_6O_4S_4$  requires C, 41.90; N, 11.27; H, 2.97; S, 17.21.  $\nu_{\max}/\text{cm}^{-1}$ : 1486–1453d (thiazole); 1255, 1139 ( $\text{SO}_2$ ); 974 (S–N). Solid UV–vis ( $\lambda_{\max}/\text{nm}$ ): 312, 559, 684(sh). ESI-MS gives a peak at  $m/z = 771$ . Conductivity measurements in dmsO:EtOH (1:4) solutions: 30.9  $\mu\text{S}/\text{cm}$ .

Complex **3** (0.206 g, 53.5%) found: C, 43.44; N, 10.83; H, 3.46; S, 16.96.  $C_{28}H_{26}Cl_2CuN_6O_4S_4$  requires C, 43.49; N, 10.86; H, 3.38; S, 16.58.  $\nu_{\max}/\text{cm}^{-1}$ : 1483–1451d (thiazole); 1275, 1137 ( $\text{SO}_2$ ); 974 (S–N). Solid UV–vis ( $\lambda_{\max}/\text{nm}$ ): 318, 576, 660sh. ESI-MS gives a peak at  $m/z = 745$ . Conductivity measurements in dmsO:EtOH (1:4) solutions: 24.7  $\mu\text{S}/\text{cm}$ .

$[\text{Cu}_2(\text{L}^4)_2(\text{OCH}_3)_2(\text{NH}_3)_2]$  (**4**) and  $[\text{Cu}_2(\text{L}^4)_2(\text{OCH}_3)_2(\text{dmsO})_2]$  (**5**) [ $\text{HL}^4 = N$ -2-(4-Methylbenzothiazole)benzenesulfonamide]. These compounds were obtained and characterized as previously reported.<sup>26</sup>

**X-ray Data Collection.**  $[\text{Cu}(\text{L}^1)_2(\text{NH}_3)_2] \cdot 2\text{MeOH}$  (**1**),  $[\text{Cu}(\text{L}^2)_2(\text{NH}_3)_2]$  (**2**), and  $[\text{Cu}(\text{L}^3)_2(\text{NH}_3)_2]$  (**3**). A black crystal, size  $0.30 \times 0.25 \times 0.10$  mm, triclinic, space group  $P\bar{1}$  (determined from the systematic absences) for complex **1**, a black crystal, size  $0.22 \times 0.16 \times 0.10$  mm, monoclinic, space group  $P_a$  for complex **2**, or a dark violet crystal, size  $0.17 \times 0.15 \times 0.12$  mm, monoclinic, space group  $P_c$  for complex **3** was used for the data collection. Data collection was performed at 200(2) K on a Nonius KappaCCD single-crystal diffractometer, using Cu–K $\alpha$  radiation ( $\lambda = 1.5418$  Å). Crystal–detector distance was fixed at 29 mm, and a total of 760 (**1**), 670 (**2**), or 766 (**3**) images were collected using the oscillation method (both  $f$  and  $w$  oscillations were necessary to fill the Ewald Sphere), with  $2^\circ$  oscillation and 40 s (**1** and **2**) or 150 s (**3**) exposure time per image. Data collection strategy was calculated with the program Collect.<sup>28</sup> Data reduction and cell refinement were performed with the programs DENZO and SCALEPACK.<sup>29</sup> A total of 7312 (**1**), 10995 (**2**), or 13350 (**3**) reflections were collected between  $\theta = 2^\circ$  and  $70^\circ$ . Unit cell dimensions were determined from 1286 (**1**), 2022 (**2**), or 2212 (**3**) reflections. Multiple measured reflections were averaged,  $R_{\text{merge}} = 0.052$ , resulting in 2568 unique reflections ( $hkl$  range  $-10 < h < 8$ ,  $-9 < k < 8$ ,  $0 < l < 17$ ), of which 2010 are observed with  $I > 2\sigma(I)$  for complex **1**,  $R_{\text{merge}} = 0.064$ , resulting in 2022 unique reflections ( $hkl$  range  $0 < h < 12$ ,  $0 < k < 14$ ,  $-12 < l < 12$ ), of which 1882 are observed with  $I > 2\sigma(I)$  for complex **2** or  $R_{\text{merge}} = 0.068$ , resulting in 2455 unique reflections ( $hkl$  range  $-14 < h < 14$ ,  $0 < k < 14$ ,  $0 < l < 12$ ), of which 2353 are observed with  $I > 2\sigma(I)$  for complex **3**. Final mosaicity was  $0.659(4)^\circ$  (**1**),  $0.596(4)^\circ$  (**2**), or  $0.624(3)^\circ$  (**3**). Data completeness was 98.7% (**1** and **2**) or 96.0% (**3**). Intensity–error ratio for all reflections was 379.4:15.8 (**1**), 397.4:18.5 (**2**), or 479.0:25.8 (**3**).

A summary of crystallographic data for complexes **1–3** is collected in Table 1.

**Structure Refinement.** Crystal structures of **1–3** were solved by Patterson methods, using the program DIRDIF-96.<sup>30</sup> Anisotropic least-squares refinement was carried out using SHELXL-97.<sup>31</sup> All

**Table 1.** Crystal Data and Structure Refinement for  $[\text{Cu}(\text{L}^1)_2(\text{NH}_3)_2] \cdot 2\text{MeOH}$  (**1**),  $[\text{Cu}(\text{L}^2)_2(\text{NH}_3)_2]$  (**2**), and  $[\text{Cu}(\text{L}^3)_2(\text{NH}_3)_2]$  (**3**)

	<b>1</b>	<b>2</b>	<b>3</b>
empirical formula	$C_{30}H_{34}CuN_8O_{10}S_4$	$C_{26}H_{22}Cl_2CuN_6O_4S_4$	$C_{28}H_{26}Cl_2CuN_6O_4S_4$
formula weight	858.43	745.18	770.95
crystal system	triclinic	monoclinic	monoclinic
space group	$P\bar{1}$	$P_a$	$P_c$
$a$ , Å	8.041(1)	12.533(1)	12.704(1)
$b$ , Å	8.176(1)	12.203(1)	12.275(1)
$c$ , Å	14.451(1)	10.466(1)	10.570(1)
$\alpha$ (deg)	90.904(1)		
$\beta$ (deg)	115.877(1)	111.62(1)	105.879(3)
$\gamma$ (deg)	92.568(1)		
$V$ , Å <sup>3</sup>	912.51(17)	1488.1(2)	1585.4(2)
$Z$	1	2	2
$\lambda$ , Å	1.54184	1.54184	1.54184
$\mu$ , mm <sup>−1</sup>	3.561	5.703	5.375
$\rho_{\text{calcd}}$ , g/cm <sup>3</sup>	1.562	1.663	1.607
$T$ , K	200(2)	200(2)	150(2)
$R_1$	0.0474	0.0446	0.0759
$wR_2$	0.1160	0.1216	0.1944

non-hydrogen atoms were anisotropically refined. All hydrogen atoms were considered as ideal and geometrically placed. All hydrogen atoms were isotropically refined. Final cycle of full-matrix least-squares refinement based on 2560 reflections and 243 parameters for complex **1**, 2022 reflections and 389 parameters for complex **2**, or 2455 reflections and 407 parameters for complex **3** converged to a final value of  $R_1$  ( $F^2 > 2\sigma(F^2)$ ) = 0.0474 (complex **1**), 0.0456 (complex **2**), or 0.0759 (complex **3**);  $wR_2$  ( $F^2 > 2\sigma(F^2)$ ) = 0.1160 (**1**), 0.1222 (**2**), and 0.1944 (**3**);  $R_1(F^2)$  = 0.0601 (**1**), 0.0486 (**2**), and 0.774 (**3**);  $wR_2(F^2)$  = 0.1252 (**1**), 0.1237 (**2**), and 0.1956 (**3**). Final difference Fourier maps showed no peaks higher than  $0.304 \text{ e } \text{Å}^{-3}$  for compound **1**,  $1.028 \text{ e } \text{Å}^{-3}$  for compound **2**, or  $1.150 \text{ e } \text{Å}^{-3}$  for compound **3** nor deeper than  $-0.478 \text{ e } \text{Å}^{-3}$  (**1**),  $-0.875 \text{ e } \text{Å}^{-3}$  (**2**), or  $-0.604 \text{ e } \text{Å}^{-3}$  (**3**).

For the three complexes atomic scattering factors were taken from the *International Tables for Crystallography* (Vol. C).<sup>32</sup>

Geometrical calculations were made using PARST.<sup>33</sup> The crystallographic plots were made using PLATON.<sup>34</sup> All calculations were performed at the University of Oviedo on the Scientific Computer Center and X-ray group computers.

**In Vitro Evaluation of SOD-like Activity.** SOD-like activity of the complexes **1–5** was determined by using the inhibition by the complexes of the reaction of  $\text{O}_2^{\cdot -}$  with nitro blue tetrazolium (NBT), following the method published by Oberley and Spitz with slight modifications.<sup>35</sup> Xanthine ( $1.5 \times 10^{-4} \text{ M}$ ) and xanthine oxidase in 50 mM potassium phosphate buffer, pH = 7.8, are used to generate a reproducible and constant flux of superoxide anions. The rate of reduction of NBT ( $5.6 \times 10^{-5} \text{ M}$ ) to blue formazane was followed spectrophotometrically at 560 nm. Data in the absence of the complex were used as a reference. The rate of NBT reduction

(30) Beurskens, P. T.; Beurskens, G.; Bosman, W. P.; de Gelder, R.; García-Granda, S.; Gould, R. O.; Israëland, R.; Smits, J. M. M. *The DIRDIF-96 Program System*; Crystallography Laboratory, University of Nijmegen: The Netherlands, 1996.

(31) Sheldrick, G. M. *SHELXL-97, A computer program for refinement of crystal structures*; University of Göttingen, 1997.

(32) *International Tables for X-ray Crystallography*; Kynoch Press: Birmingham (Present distributor: Kluwer Academic Publishers: Dordrecht, The Netherlands), 1974.

(33) Nardelli, M. *Comput. Chem.* **1983**, *7*, 95.

(34) Spek, A. L. *PLATON, A Multipurpose Crystallographic Tool*; Utrecht University: Utrecht, The Netherlands, 2000.

(35) Oberley, L. W.; Spitz, D. R. In *Handbook of Methods for Oxygen Radicals Research*; Greenwald, R. A., Ed.; CRC Press: Boca Raton, FL, 1986; p 217.

(28) Nonius, B. V. *Collect* 1997–2000.

(29) Otwinowski, Z.; Minor, W. *Methods Enzymol.* **1997**, *276*, 307.



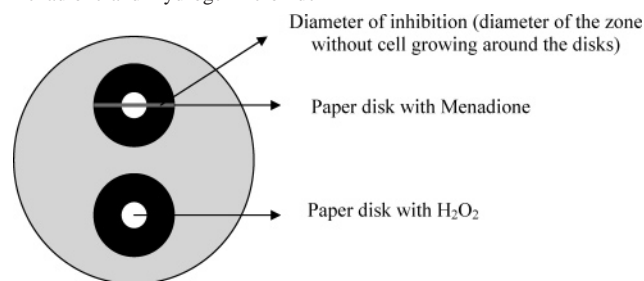
was progressively inhibited after the addition of copper complex solutions at increasing concentrations prepared in 50 mM Tris-HCl buffer (pH = 7.8) to the system. The percentage inhibition of the NBT reduction was used as a measure of the SOD activity of the compounds. In a typical experiment 0.1 mL of xanthine oxidase was added to 0.8 mL of a solution containing 0.69 mL of potassium phosphate buffer (pH = 7.8), 0.025 mL of NBT, and 0.085 mL of xanthine. The enzymatic system was also tested against a possible inactivation caused by the copper(II) complexes. To evaluate if the complexes affect the generation of superoxide anions by directly interacting with the enzymatic system, the formation of uric acid from xanthine was followed at 310 nm. The inhibition percentage of enzyme activity was subtracted from that of NBT. The concentration of complex required to yield 50% inhibition of NBT reduction (named IC<sub>50</sub>) was determined from a plot of percentage inhibition versus complex concentration. The IC<sub>50</sub> data have been calculated from the mean of three independent measurements.

**In Vivo Evaluation of the SOD-like Activity.** The in vivo SOD-like activity of the complexes **1–5** was evaluated over three different strains of *S. cerevisiae*: W303-1A, wild type (*MATa ade2-1 ura3-1 his3-11 trp1 leu2-3 leu2-112 can1-100*), ATCC96687, strain defective in the cytoplasmatic copper-dependent SOD (*MATa ura3-52 trp1-289 his3-Δ1 leu2-3 leu2-112 sod1::URA3*), and ATCC96688, strain defective in the mitochondrial manganese dependent SOD (*MATa ura3-52 trp1-289 his3-Δ1 leu2-3 leu2-112 sod2::TRP1*). The strains were obtained from American Type Culture Collection (ATCC). The protective action of the complexes against free radicals produced by respiration and against free radicals generated by menadione or H<sub>2</sub>O<sub>2</sub> was determined.

**Evaluation of the Protective Effect of the Complexes against Free Radicals Produced by Respiration.** Solutions of the complexes **1–5** (30, 50, 70, or 90 μM) in dmsO:EtOH (1:4) were added to 15 mL of melted YPgly medium (1% yeast extract, 2% peptone, 2% glycerol, 1.5% agar, and 2% ethanol), which was kept at 45 °C. Media were poured in Petri plates and allow to solidify at room temperature. Cell cultures were grown aerobically overnight at 28 °C in stirred liquid YPD reach medium (1% yeast extract, 2% peptone, and 2% glucose). Drops of 5 μL of the three strains at decreasing dilutions (10<sup>-2</sup>, 10<sup>-3</sup>, 10<sup>-4</sup>, 10<sup>-5</sup>, and 10<sup>-6</sup>) obtained from an overnight culture were poured in the Petri dishes and were incubated at 28 °C for 4 days. Untreated cultures were incubated in parallel. The increased growth of cells found in the presence of the copper(II) compounds compared with cell growth in the absence of the complexes was taken as a qualitative estimate of the protective effect based on serial dilution drops assays. Experiments were performed three times.

**Evaluation of the Protective Effect of the Complexes against Free Radicals Produced by Oxidative Agent.** Yeast cells were grown in YPD reach medium (1% yeast extract, 2% peptone, and 2% glucose). Solid media contained 1.5% agar. Cell density from overnight cultures was determined by cell counting in a "Nebauer" hematimeter. A total of 10<sup>6</sup> cells were resuspended in 15 mL of melted solid YPD media, which was kept at 45 °C. Solutions of the complexes in dmsO:EtOH (1:4) at increasing concentrations (30, 50, or 70 μM) were added to the growth medium. Cell suspensions were poured in Petri dishes and allow to solidify at room temperature. Paper disks 6 mm in diameter (Antibiotica test Blättchen) containing 15 μL of a 40 mM menadione solution in ethanol or 5 μL of H<sub>2</sub>O<sub>2</sub> (35%) for wild and Δ*sod2* strains were placed over the media. For Δ*sod1* strain the paper disks contained 5 μL of a 5 mM menadione solution in ethanol or 5 μL of H<sub>2</sub>O<sub>2</sub> (17.5%). Differences in the amounts of oxidants used depended on the differences in sensibility of the different strains.<sup>36</sup> Cultures

**Scheme 2.** Diameter of Inhibition around the Paper Disks Containing Menadione and Hydrogen Peroxide



were incubated at 28 °C for 72 h. Diameters of the inhibition area (zone without cell growing around the disks) were measured and were taken as a quantitative estimate of the protective action (see Scheme 2). The final data have been calculated as the media of three independent measurements.

**Toxicity Assays.** Before examination of the protective action of the compounds against free radicals, their putative toxicity over the wild, Δ*sod1*, and Δ*sod2* strains of *S. cerevisiae* was determined following the procedure previously described.<sup>11</sup>

### 3. Results and Discussion

**3.1. Crystal Structure.** The crystal structures with the atomic numbering scheme of compounds **1**, **2**, and **3** are shown in Figures 1, 2, and 3, respectively. Significant bond lengths and angles are listed in Table 2. In [Cu(L<sup>1</sup>)<sub>2</sub>(NH<sub>3</sub>)<sub>2</sub>]·2MeOH (**1**) the copper ion is four-coordinated in a slightly distorted square planar environment. The copper(II) is linked to the benzothiazole N2 and N2#1 atoms from two sulfonamidate anions and to the N4 and N4#1 atoms from two NH<sub>3</sub> molecules. The Cu–N<sub>benzothiazole</sub> distances are 1.975(3) Å and the Cu–N<sub>ammonia</sub> ones are 2.003(3) Å. The benzothiazole nitrogen atoms are in trans position. The bond angles in the CuN<sub>4</sub> chromophore are nearly regular, ranging from 89.52(12)° to 90.48(12)°. Tetrahedrality, for any tetracoordinate copper complexes, can be characterized by the angle subtended by two planes, each encompassing the copper and two adjacent donor atoms.<sup>37</sup> For strictly square planar complexes with *D*<sub>4h</sub> symmetry, the tetrahedrality is 0°. For tetrahedral complexes with *D*<sub>2d</sub> symmetry, the tetrahedrality equals 90°. The value of the dihedral angle for complex **1** is 0°, indicating that the complex geometry is square planar.

Two uncoordinated methanol molecules stabilize the crystal structure through moderate intermolecular hydrogen bonds<sup>38</sup> between the ammonia nitrogen and the methanol oxygen [N4...O5 3.0228 Å, 142.70°], and between the methanol oxygen and the sulfonamide oxygen [O5...O4 2.8273 Å, 159.32°]. Also, there are some weak hydrogen bonds between the ammonia nitrogen and the oxygen of the NO<sub>2</sub> group.

The geometrical environment of the metal ion in [Cu(L<sup>2</sup>)<sub>2</sub>(NH<sub>3</sub>)<sub>2</sub>] (**2**) is distorted square planar. Cu(II) is coordinated by four nitrogen atoms: two ammonia nitrogen atoms and

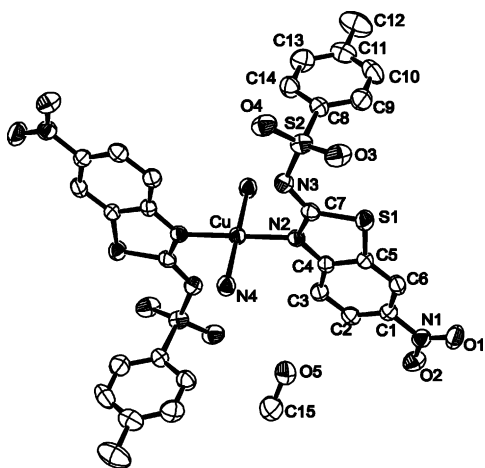
(36) Jamienson, D. J.; Rivers, S. L.; Stephen, W. S. *Microbiology* **1994**, *140*, 3277.

(37) Battaglia, L. P.; Bonamartini-Corradi, A.; Marcotrigiano, G.; Menabue, L.; Pellacani, G. C. *Inorg. Chem.* **1979**, *18*, 148.

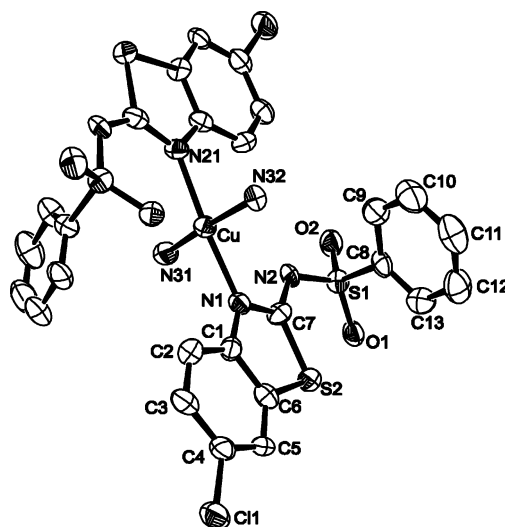
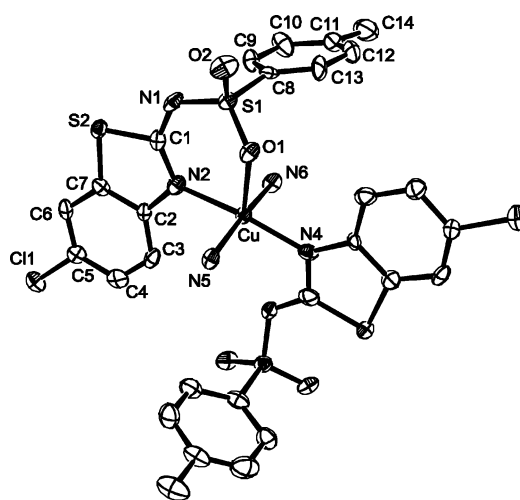
(38) Jeffrey, G. A. *An Introduction to Hydrogen Bonding*; Oxford University Press: Oxford, 1997.

**Table 2.** Selected Bond Lengths (Å) and Angles (°) for [Cu(L<sup>1</sup>)<sub>2</sub>(NH<sub>3</sub>)<sub>2</sub>] $\cdot$ 2MeOH (**1**), [Cu(L<sup>2</sup>)<sub>2</sub>(NH<sub>3</sub>)<sub>2</sub>] (**2**), and [Cu(L<sup>3</sup>)<sub>2</sub>(NH<sub>3</sub>)<sub>2</sub>] (**3**)<sup>a</sup>

[Cu(L <sup>1</sup> ) <sub>2</sub> (NH <sub>3</sub> ) <sub>2</sub> ] $\cdot$ 2MeOH		[Cu(L <sup>2</sup> ) <sub>2</sub> (NH <sub>3</sub> ) <sub>2</sub> ]		[Cu(L <sup>3</sup> ) <sub>2</sub> (NH <sub>3</sub> ) <sub>2</sub> ]	
Cu1–N2	1.975(3)	Cu1–N1	2.014(7)	Cu1–N5	2.000(9)
Cu1–N2#1	1.975(7)	Cu1–N21	2.029(7)	Cu1–N4	2.000(10)
Cu1–N4#1	2.003(3)	Cu1–N32	2.082(8)	Cu1–N2	2.023(9)
Cu1–N4		Cu1–N31	2.217(8)	Cu1–N6	2.024(8)
				Cu1–O1	2.269(7)
N2–Cu1–N2#1	180.0	N1–Cu1–N21	171.8(3)	N5–Cu1–N4	90.0(4)
N2–Cu1–N4#1	89.52(12)	N1–Cu1–N32	89.7(3)	N5–Cu1–N2	89.2(4)
N2#1–Cu1–N4#1	90.48(12)	N21–Cu1–N32	93.0(3)	N4–Cu1–N2	172.5(4)
N2–Cu1–N4	90.48(12)	N1–Cu1–N31	90.8(3)	N5–Cu1–N6	170.1(4)
N2#1–Cu1–N4	89.52(12)	N21–Cu1–N31	85.4(3)	N4–Cu1–N6	88.8(4)
N4#1–Cu1–N4	180.0	N32–Cu1–N31	171.2(3)	N2–Cu1–N6	90.7(4)
				N5–Cu1–O1	86.9(3)
				N4–Cu1–O1	101.7(3)
				N2–Cu1–O1	85.7(3)
				N6–Cu1–O1	103.0(3)

<sup>a</sup> Symmetry transformations #1  $-x, -y, -z$ .**Figure 1.** ORTEP drawing of the [Cu(L<sup>1</sup>)<sub>2</sub>(NH<sub>3</sub>)<sub>2</sub>] $\cdot$ 2MeOH (**1**).

two benzothiazole nitrogen atoms from the two sulfonamidate ligands. The Cu(II)–N<sub>ammonia</sub> coordinative bonds are significantly different [2.217(8) and 2.082(8) Å]. The Cu–N<sub>benzothiazole</sub> lengths [2.014(7) and 2.029(7) Å] are slightly longer than those obtained for the compound described before. Distortion of the ideal square-planar geometry can be inferred from the bond angles that deviate from 90° [85.4(3)–93.9(3)]. The tetrahedrality value of 11.55° suggests a slight distortion from the square-planar geometry. In the crystal packing, moderate hydrogen bonds between the ammonia nitrogen and the sulfonamide nitrogen [N3...N2, 3.3186 Å, 140.35°] and between the ammonia nitrogen and the sulfonamide oxygen [N32...O22, 3.0127 Å, 169.61°] stabilize the structure. The crystal structure of [Cu(L<sup>3</sup>)<sub>2</sub>(NH<sub>3</sub>)<sub>2</sub>] (**3**) contains a CuN<sub>4</sub>O entity in slightly distorted square-pyramidal geometry. In the basal plane the copper(II) ion is coordinated by two benzothiazole nitrogen atoms from two different sulfonamidate ligands at 2.000(9) and 2.000(10) Å and by two ammonia nitrogen atoms at 2.023(9) and 2.024(8) Å. The axial site is occupied by a sulfonamide oxygen atom of one of the sulfonamidate ions at much longer distance, 2.269(7) Å. The Cu–N<sub>benzothiazole</sub> lengths are similar and comparable to those found in **1**, **2**, and other related compounds.<sup>10,12</sup> The cis N–Cu–N angles in the equatorial plane that range from 88.8(4)° to 90.7(4)° do not deviate significantly from the ideal ones. The  $\tau$  value

**Figure 2.** ORTEP drawing of the [Cu(L<sup>2</sup>)<sub>2</sub>(NH<sub>3</sub>)<sub>2</sub>] (**2**).**Figure 3.** ORTEP drawing of the [Cu(L<sup>3</sup>)<sub>2</sub>(NH<sub>3</sub>)<sub>2</sub>] (**3**).

of 0.04 [ $\tau = (\alpha - \beta/60)$ ]<sup>39</sup> indicates a small distortion from a regular square-pyramidal geometry. The  $T^5$  parameter ( $T = \text{mean in-plane Cu–L bond distance}/\text{mean out-of-plane Cu–L bond distance}$ )<sup>40</sup> has a value of 0.88.

(39) Addison, A. W.; Rao, T. N.; Reedijk, J.; van Rijn, J.; Verschoor, C. G. *J. Chem. Soc., Dalton Trans.* **1984**, 1349.

In complexes **1** and **2** the sulfonamidate anions behave as monodentate ligands through the benzothiazole nitrogen atom. By contrast, the sulfonamidate anions in complex **3** present two different coordination behaviors. One sulfonamidate ion acts as a monodentate ligand through the benzothiazole nitrogen and the other as a bidentate ligand via the benzothiazole nitrogen and the sulfonamide oxygen. According to the coordination, the distance S1–O1 (1.472(8) Å) is markedly longer than the S1–O2 one (1.421(8) Å). The same behavior of the sulfonamide as monodentate and bidentate ligands has been found in the related complexes [Cu(L<sup>2</sup>)<sub>2</sub>(dmsO)<sub>2</sub>] and [Cu(L<sup>3</sup>)<sub>2</sub>(dmsO)<sub>2</sub>].<sup>12</sup>

**3.2. Spectroscopic Properties.** The IR spectra of **1**, **2**, and **3** present a similar pattern. With respect to the IR spectra of the ligands the following modifications are found: (i) the band corresponding to the stretching vibration of the thiazole ring is markedly shifted from 1550 cm<sup>-1</sup> in the free ligands to 1455 cm<sup>-1</sup> in the complexes, (ii) the  $\nu(\text{SO}_2)_{\text{as}}$  and  $\nu(\text{SO}_2)_{\text{s}}$  bands in the complexes are shifted to lower frequencies, and (iii) the characteristic band corresponding to the  $\nu(\text{S}-\text{N})$  appears near 975 cm<sup>-1</sup>, changed ca. 15–20 cm<sup>-1</sup> to higher frequencies. In general, the IR spectra are similar to those of other copper *N*-sulfonamide compounds.<sup>10–12,26</sup> Independently of the coordination behavior of the ligands, changes of the IR characteristic bands are found to be the same because the modifications are mainly due to the sulfonamide deprotonation.

The diffuse reflectance spectrum of complex **1** shows a broad and intense band at about 400 nm and a shoulder at about 600 nm, that correspond to a ligand-to-metal charge-transfer (LMCT) and d–d transitions, respectively. The spectrum agrees well with the coordination polyhedron shown in the crystal structure. The reflectance spectra of complexes **2** and **3** show a shoulder at 407 (complex **2**) and at 415 (complex **3**) nm and a broad band at 556 (complex **2**) and at 568 (complex **3**) nm that can be attributed to a LMCT and to a d–d transition, respectively. It is noteworthy that both complexes present similar spectra despite their coordination geometry that is distorted square planar in complex **2** and distorted square-pyramidal in complex **3**. This is probably because of the large Cu–O<sub>sulfonamidate</sub> bond distance. So, the fifth coordination atom (O<sub>sulfonamidate</sub>) has a slight influence. The difference between the spectra of complexes **1** and **2** must be due to the high square planar distortion of the latter as is shown in the crystal structures.

The UV–vis spectra of the three complexes in dmsO:EtOH (1:4) solutions used in the biological assays show a very weak d–d band at about 600 nm similar to that found in diffuse reflectance spectra.

The conductivity measurements of the three complexes in dmsO:EtOH (1:4) solution suggest that the three complexes are partially dissociated, showing conductivity values between nonelectrolyte and 1:1 electrolyte types.<sup>41</sup> These values are indicative of a mixture of the complex and a species in which one of the ligands was dissociated.

The electrospray data of these solutions show the molecular peak and another peak with a molecular mass corresponding to a species with one ligand and solvent molecule such as [CuL(NH<sub>3</sub>)<sub>2</sub>(solvent)<sub>*n*</sub>]<sup>+</sup>. Moreover, the ESI-MS spectra of the dinuclear compounds **4** and **5** in dmsO:EtOH (1:4) were obtained. The spectra display peaks at *m/z* = 830 and 952, respectively, corresponding to the molecular ones showing that the complex entities remain in solution.

**3.3. Magnetic Properties and EPR Spectra.** The room-temperature magnetic moments of complexes **1** ( $\mu_{\text{eff}} = 1.75 \mu_{\text{B}}$ ), **2** ( $\mu_{\text{eff}} = 1.73 \mu_{\text{B}}$ ), and **3** ( $\mu_{\text{eff}} = 1.78 \mu_{\text{B}}$ ) are consistent with the presence of a single unpaired electron.

The polycrystalline X-band EPR spectrum at room temperature of complex **1** is axial. The EPR parameters obtained by simulation<sup>42</sup> are  $g_{\parallel} = 2.27$ ,  $g_{\perp} = 2.05$ , and  $A_{\parallel} = 172 \times 10^{-4} \text{ cm}^{-1}$ . The quotient  $g_{\parallel}/A_{\parallel}$  is a measure for the degree of tetrahedral distortion. This quotient ranges from ca. 105 to 135 cm for square planar structures.<sup>43</sup> The  $g_{\parallel}/A_{\parallel}$  value of 132 cm of compound **1** agrees well with the almost regular square planar geometry found in the crystal structure.

For complex **2** the EPR spectrum is rhombic. The parameters calculated by simulation,  $g_3 = 2.20$ ,  $g_2 = 2.06$ , and  $g_1 = 2.03$ , correlate well with the geometrical distortion found in the crystal structure. The *R* value<sup>44</sup> [ $R = (g_2 - g_1)/(g_3 - g_2)$ ] of 0.2 indicates that the unpaired electron is in the  $d_{x^2-y^2}$  orbital.

The axial spectrum of complex **3** presents values of  $g_{\parallel} = 2.22$  and  $g_{\perp} = 2.05$ , which are characteristic of the geometry deduced from crystallographic data.

**3.4. SOD-like Activity. In Vitro Superoxide Dismutase-like Activity.** The superoxide dismutase activity of the monomeric complexes **1–3** and the dimeric complexes [Cu<sub>2</sub>(L<sup>4</sup>)<sub>2</sub>(OCH<sub>3</sub>)<sub>2</sub>(NH<sub>3</sub>)<sub>2</sub>] (**4**) and [Cu<sub>2</sub>(L<sup>4</sup>)<sub>2</sub>(OCH<sub>3</sub>)<sub>2</sub>(dmsO)<sub>2</sub>] (**5**) [HL<sup>4</sup> = *N*-2-(4-methylbenzothiazole)benzenesulfonamide] previously reported<sup>26</sup> was assayed by their ability to inhibit the reduction of nitro blue tetrazolium. By way of comparison, the activity of CuCl<sub>2</sub>·2H<sub>2</sub>O was assayed under the same conditions. The superoxide scavenging data indicate that complexes **1–3** exhibit high activity, similar to those of complexes with related benzothiazole sulfonamide ligands and higher than the activity of copper sulfathiazole complexes (Table 3).<sup>10–15</sup> Their IC<sub>50</sub> values are 0.244(±0.041), 0.181(±0.002), and 0.182(±0.010) μM, respectively. Complexes **4** and **5** clearly show higher superoxide dismutase activity [IC<sub>50</sub> = 0.103(±0.007) and 0.059(±0.001) μM, respectively] compared with the other three complexes. It is interesting to note that the activity exhibited by complexes **4** and **5** is only 17 and 10 times, respectively, less than that of the native enzyme. These results seem to indicate that the dimer nature increases the ability of the compounds to dismutate the superoxide radical. In fact, the most active compounds in vitro found in the literature are dinuclear complexes.<sup>45</sup> In

(40) Matović, Z. D.; Pelosi, G.; Ianelli, S.; Ponticelli, G.; Radanović, D. D.; Radanović, D. J. *Inorg. Chim. Acta* **1998**, 268, 221.

(41) Geary, *Coord. Chem. Rev.* **1971**, 7, 81.

(42) WINEPR–Simfonia. 1.25; Bruker Analytik GmG: Karlsruhe, FRG, 1994–1996.

(43) Sakaguchi, U.; Addison, W. A. *J. Chem. Soc., Dalton Trans.* **1978**, 600.

(44) Hathaway, B. J.; Duggan, M.; Murphy, A.; Mullane, J.; Power, C.; Walsh, A.; Walsh, B. *Coord. Chem. Rev.* **1981**, 36, 267.



**Table 3.** IC<sub>50</sub> (μM) Values of Copper Complexes<sup>a</sup>

complex	IC <sub>50</sub>	ref.
[Cu(L <sup>1</sup> ) <sub>2</sub> (NH <sub>3</sub> ) <sub>2</sub> ]·MeOH ( <b>1</b> )	0.244	this work
[Cu(L <sup>2</sup> ) <sub>2</sub> (NH <sub>3</sub> ) <sub>2</sub> ] ( <b>2</b> )	0.181	this work
[Cu(L <sup>3</sup> ) <sub>2</sub> (NH <sub>3</sub> ) <sub>2</sub> ] ( <b>3</b> )	0.182	this work
[Cu <sub>2</sub> (L <sup>4</sup> ) <sub>2</sub> (OCH <sub>3</sub> ) <sub>2</sub> (NH <sub>3</sub> ) <sub>2</sub> ] ( <b>4</b> )	0.103	this work
[Cu <sub>2</sub> (L <sup>4</sup> ) <sub>2</sub> (OCH <sub>3</sub> ) <sub>2</sub> (dmsO) <sub>2</sub> ] ( <b>5</b> )	0.059	this work
[Cu(L <sup>2</sup> ) <sub>2</sub> (dmsO) <sub>2</sub> ]	0.188	12
[Cu(en) <sub>2</sub> ](L <sup>3</sup> ) <sub>2</sub>	0.344	10
[Cu(L <sup>4</sup> ) <sub>2</sub> (py) <sub>2</sub> ]	0.146	11
[Cu(L <sup>5</sup> ) <sub>2</sub> (py) <sub>2</sub> ]	0.172	11
[Cu(stz)(py) <sub>3</sub> Cl]	1.310	13
[Cu(Hstz)(MeOH)Cl <sub>2</sub> ]	2.510	13
[Cu(stz) <sub>2</sub> (Him) <sub>2</sub> ]MeOH	0.664	14
[Cu(stz) <sub>2</sub> (4,4-dmHim) <sub>2</sub> ]	0.742	15
[Cu(stz) <sub>2</sub> (1,2-dmHim) <sub>2</sub> ]	1.03	15
[Cu(stz) <sub>2</sub> (4-mHim) <sub>2</sub> ]	0.586	15
Cu <sub>2</sub> Zn <sub>2</sub> SOD	0.006	11

<sup>a</sup> Abbreviations: HL<sup>1</sup> = *N*-2-(4-methylphenylsulfamoyl)-6-nitro-benzothiazole; HL<sup>2</sup> = *N*-2-(phenylsulfamoyl)-6-chloro-benzothiazole; HL<sup>3</sup> = *N*-2-(4-methylphenylsulfamoyl)-6-chloro-benzothiazole; HL<sup>4</sup> = *N*-2-(phenylsulfamoyl)-4-methyl-benzothiazole; HL<sup>5</sup> = *N*-2-(naphthalenesulfamoyl)-6-nitro-benzothiazole; Hstz = sulfathiazole (4-amino-*N*-2-thiazolylbenzenesulfonamide); Him = imidazole; 4,4-dmHim = 4,4-dimethylimidazole; 1,2-dmHim = 1,2 dimethylimidazole; 4-mHim = 4-methylimidazole; py = pyridine.

this sense, nuclearity could play an important role in the SOD-like activity exhibited by our complexes in vitro. The IC<sub>50</sub> values of the five complexes are lower than that of Cu(II) [IC<sub>50</sub> = 0.450(±0.015) μM], indicating that their activity is not due to a dissociation of the complexes.

It has been found that a more distorted geometry leads to higher SOD activity.<sup>46</sup> In good agreement with this, complex **1** (that has the less distorted copper environment) presents the lower activity.

Also, it is remarkable that, despite the different coordination polyhedra of compounds **2** and **3**, their IC<sub>50</sub> values are almost coincident. The similar SOD activity of the complexes can be explained considering that both complexes present limited steric hindrance and vacant coordination sites that permit the access and the successful binding of the O<sub>2</sub><sup>•−</sup> radical. Moreover, a favorable response of π-electrons of the aromatic side chain could stabilize the Cu–O<sub>2</sub><sup>•−</sup> interactions. Furthermore, the binding of the sulfonamide to copper(II) is important to obtain complexes with high SOD activity because previous related complexes<sup>10</sup> in which the sulfonamide acts as a contra-ion presented lower activity than the complexes presented in this work (Table 3).

**In Vivo SOD-like Activity.** As has been shown the synthesized complexes exhibit high SOD activity measured in vitro. However, the ability to dismutate the superoxide anions in vitro is not enough to be a SOD mimic in vivo. Assays with mutants of the yeast *S. cerevisiae* were carried out to determine the SOD activity in a biological system.

Previously, the presence of the complexes in solution was confirmed by ESI-MS as described in section 3.2.

Before evaluation of the in vivo superoxide dismutase mimetic activity of the complexes, their putative toxicity was

determined by a previously reported method.<sup>11</sup> The results show that complexes do not present significant toxicity at the assayed concentrations (30, 50, 70, and 90 μM) (data not shown).

To quantify the in vivo SOD-like activity of the Cu(II) complexes we have employed a method recently developed by our research group, based on the protection provided by the compounds against free radicals over *S. cerevisiae* strains (the copper defective *Δsod1* mutant and the manganese defective *Δsod2* mutant).<sup>11</sup> The protective effect of the complexes against both free radicals produced in the respiration and against free radicals generated by oxidative agents (hydrogen peroxide or menadione) has been tested.

#### Complex Protection against Endogenous Free Radicals.

A low level of superoxide radicals is constantly generated by aerobic respiration. The electron-transport chain of mitochondria, which is meant to escort four electrons to molecular oxygen to form water, occasionally leaks a single electron and it is a constant source of radicals. Free radical reactions produced death in cells due to their ability to damage a large number of cellular constituents, especially the defective SOD cells which are more sensitive.

To evaluate the protective effect of complexes **1–5** against free radicals generated in respiration, three strains of *S. cerevisiae*, wild, *Δsod1*, and *Δsod2*, were grown in a medium with glycerol, which is a nonfermentable carbon source for *S. cerevisiae*. Figure 4 shows the growth of dilutions 10<sup>−2</sup>, 10<sup>−3</sup>, 10<sup>−4</sup>, 10<sup>−5</sup>, and 10<sup>−6</sup> (obtained from an overnight culture) of the three strains treated with increasing concentrations of complexes **1–5**.

As expected, the growth of the wild strain is not significantly modified by the complexes because this strain keeps both mitochondrial MnSOD and cytoplasmatic Cu<sub>2</sub>-Zn<sub>2</sub>SOD enzymes (Figure 4). Similar behavior is observed in the *Δsod2* strain because this strain contains the cytoplasmatic Cu<sub>2</sub>Zn<sub>2</sub>SOD enzyme.

All the complexes are able to protect the *Δsod1* strain. The protective effect of the complexes on the *Δsod1* strain is found to be significant and much higher than the copper salt protective effect. In particular, 70 and 90 μM concentrations of complex **1** produce an almost complete recuperation of *Δsod1* strain and its growth is indistinguishable from that of the wild strain. The activity of complexes **2–5** (similar to that of the previously reported complexes)<sup>11,12</sup> is lower than that of complex **1** but higher than the CuCl<sub>2</sub> activity. It is remarkable that the protective effect of the dimeric complexes **4** and **5** is not higher than that of the monomeric ones, although their activities, determined by the indirect method, were more elevated.

From these results we can conclude that the five complexes are able to penetrate into the cells and protect them against the free radicals produced in respiration processes by compensation for the Cu<sub>2</sub>Zn<sub>2</sub>SOD. In particular, complex **1**, which is the most effective, can be considered a promising protective agent against toxicity of oxidative stress.

#### Complex Protection against Exogenous Free Radicals.

To evaluate the protective effect of complexes **1–5** against exogenous free radicals, the *Δsod1* strain was grown in a

(45) Tabbi, G.; Driessen, W. L.; Reedijk, J.; Bonomo, R. P.; Veldman, N.; Spek, A. L. *Inorg. Chem.* **1997**, *36*, 1168.

(46) Bonomo, R. P.; Conte, E.; Impellizzeri, G.; Pappalardo, G.; Purrello, R.; Rizzarelli, E. *J. Chem. Soc., Dalton Trans.* **1996**, 3093.

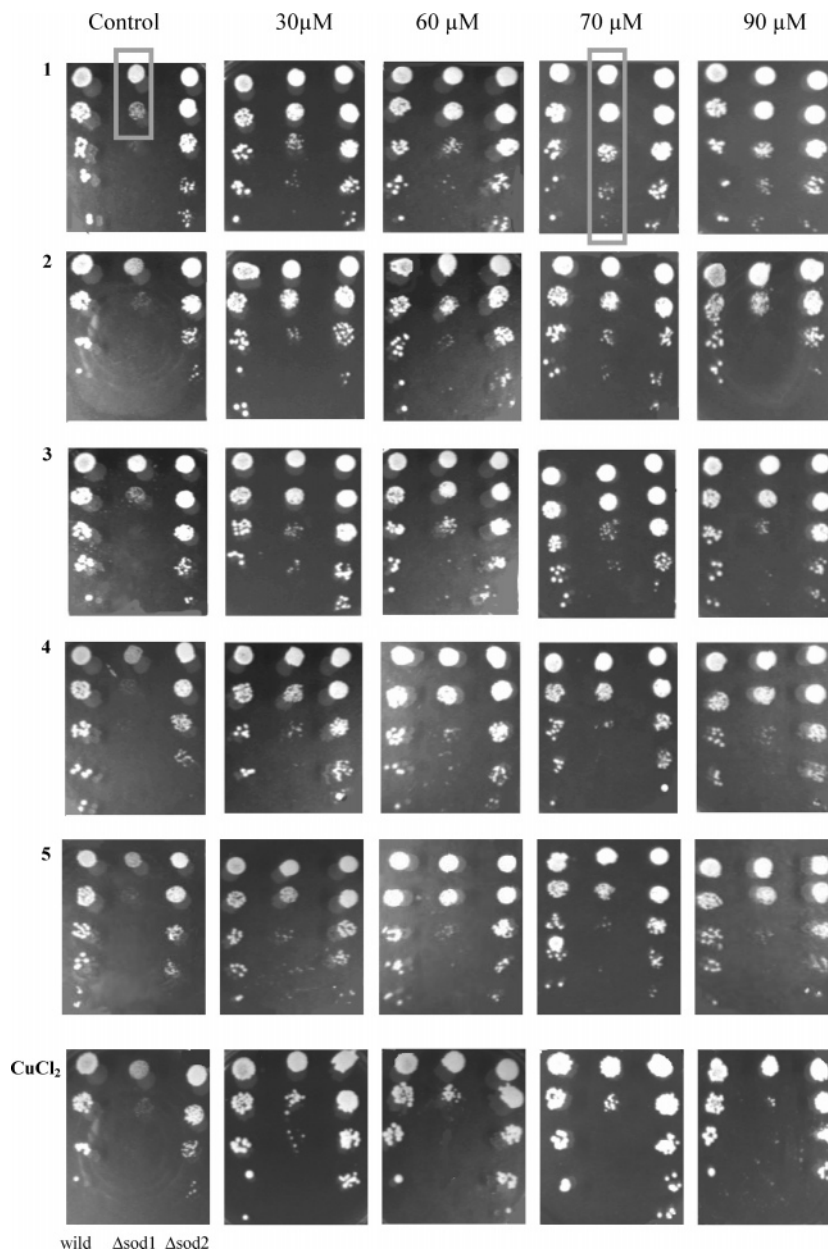


**Figure 4.** Effect of complexes **1–5**, and CuCl<sub>2</sub> on the growth of the *Saccharomyces cerevisiae* against free radicals produced by respiration. In each panel the first column represents a wild strain; the second column represents the  $\Delta sod1$  mutant; the third column represents the  $\Delta sod2$  mutant. In each column; strains are shown at decreasing dilutions:  $10^{-2}$ ,  $10^{-3}$ ,  $10^{-4}$ ,  $10^{-5}$ , and  $10^{-6}$ .

culture containing glucose. In this medium the initial metabolic pathway is fermentation. The source of free radicals is the oxidative stress inducers, menadione or  $\text{H}_2\text{O}_2$ . Menadione (paper disks at the top of each Petri dish) (see Scheme 2) generates  $\text{O}_2^{\bullet-}$  and  $\text{H}_2\text{O}_2$  (paper disks at the bottom) produces  $\bullet\text{OH}$ . The results are given in Figure 5 which shows the growth inhibition area (black region around the disk) of the  $\Delta\text{sod1}$  strain produced by the oxidative agents with different concentrations of complex 1–5. By comparison, both the wild and the  $\Delta\text{sod2}$  mutant strains, which share the copper-dependent SOD, were also studied (data not shown).

In the presence of the five complexes, a growth increase is observed for the  $\Delta sodI$  strain (smaller diameter of the inhibition area) at 30, 50, and 70  $\mu\text{M}$  complex concentrations.

This result clearly suggests that the complexes provide protection against the oxidative stress generated by both menadione and H<sub>2</sub>O<sub>2</sub>. This protective effect does not depend significantly on complex concentration. The protective action against O<sub>2</sub><sup>•−</sup> produced by menadione is higher than the protection against •OH generated by H<sub>2</sub>O<sub>2</sub>. Of special relevance is that complexes **4** and **5** do not have a higher activity than the other complexes assayed, in contrast to the expectation from their IC<sub>50</sub> values obtained in vitro.

These assays have been performed with CuCl<sub>2</sub> under the same conditions. In the presence of CuCl<sub>2</sub> it is possible to observe a reduction of the diameter of the inhibition area for the *ΔsodI* strain but this reduction is lower than that in the presence of the complexes. These results are summarized in Figure 6 that represent the percent of reduction of the



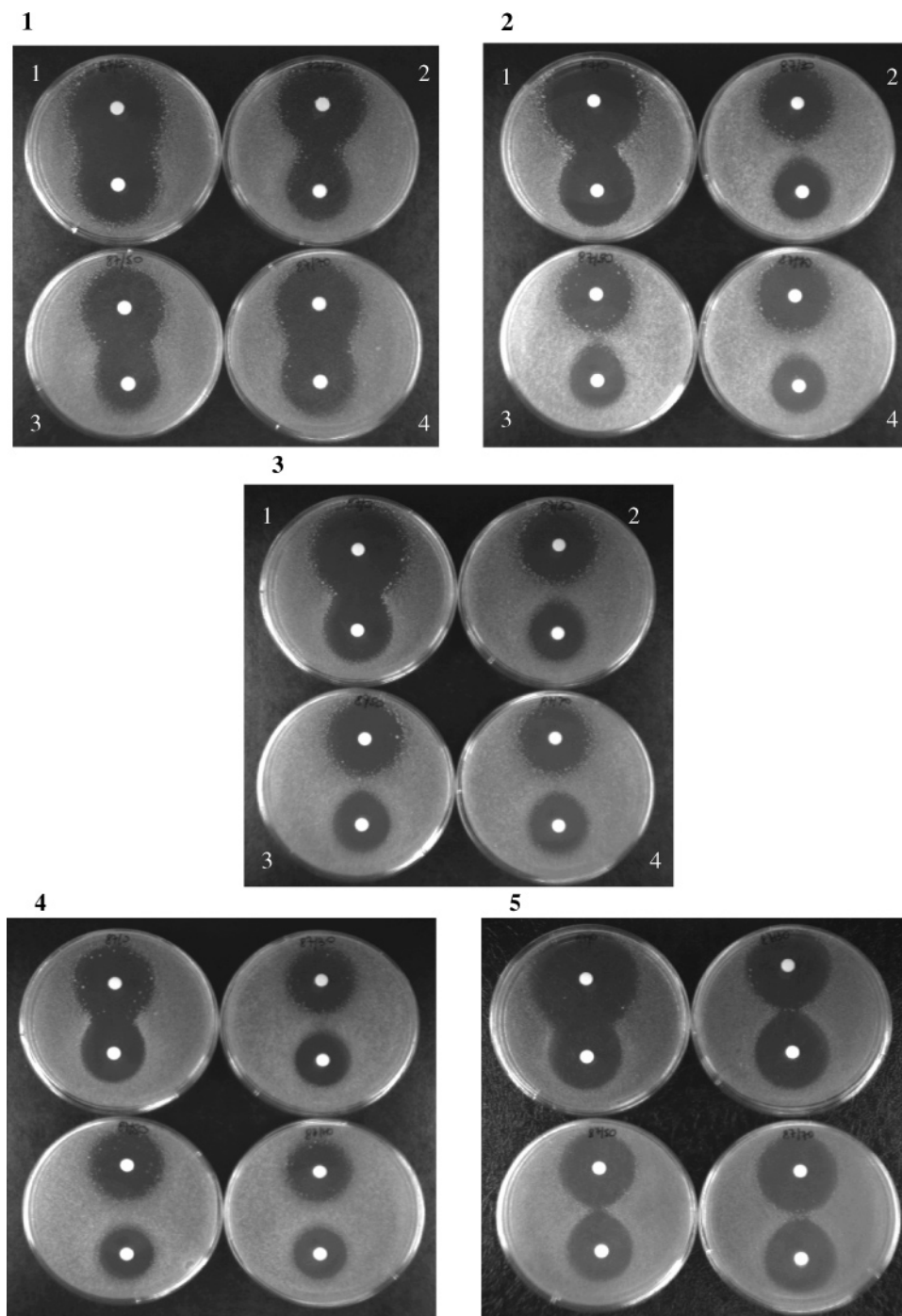


**Figure 5.** Effect of complexes **1–5** on the growth of the  $\Delta\text{sod1}$  mutant against free radicals produced by menadione (paper disk at the top of each Petri dish) and  $\text{H}_2\text{O}_2$  (paper disk at the bottom of each Petri dish). For each photograph, 1 is the control; 2 is the  $30\ \mu\text{M}$  complex; 3 is the  $50\ \mu\text{M}$  complex; 4 is the  $70\ \mu\text{M}$  complex.

diameter of the growth inhibition area produced by the five complexes at  $50\ \mu\text{M}$  and by  $\text{CuCl}_2$  at the same concentration when the oxidative stress is produced by menadione. It is possible to deduce that the protective effect of the complexes is higher than the protection produced by the copper salt. Also, it is noteworthy that the reduction of the inhibition diameter produced by complex **2** or **3** is double that of copper(II).

As expected, no protection effect of the five complexes or  $\text{CuCl}_2$  was observed in either the wild type or the  $\Delta\text{sod2}$

strains (data not shown), since both strains have the copper-dependent SOD.

The results obtained from these assays clearly demonstrate that, at least in the range of the concentrations tested, the complexes **1–5** show SOD-like activity in vivo higher than that of  $\text{Cu(II)}$ . The protective action of **1–5** is similar to that shown by previously reported complexes with related sulfonamide ligands.<sup>11,12</sup>

In conclusion, the dimer complexes are more effective than the monomer ones in vitro. However, the in vivo activity of

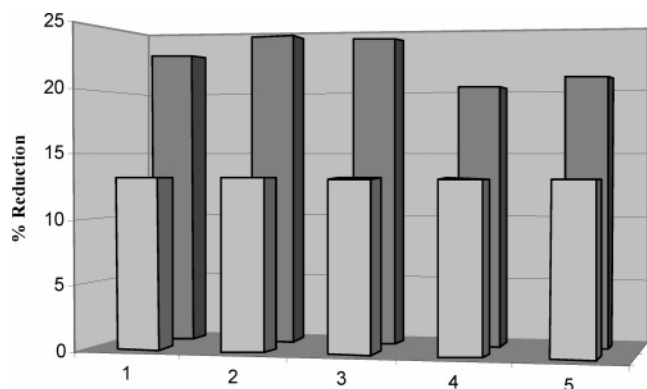


**Figure 6.** Percentage reduction of the diameter of the growth inhibition area of 50  $\mu$ M complexes **1–5** (dark color), and CuCl<sub>2</sub> (light color) when oxidative stress was produced by menadione.

the dimer complexes is lower than that of the monomer ones. Therefore, it could be deduced that in vivo some physiological factors (lipophilicity, ability of the complexes to cross the

cellular structures, enzymatic activity, detoxifying mechanisms, etc.) must be involved in the activity of our complexes. In particular, we consider that the lower activity of the dinuclear compounds in respect to the mononuclear ones is due to their bulky size that hinders them, to some extent, from crossing the cellular membrane.

**Acknowledgment.** J.B. and G.A. acknowledge financial support from the Spanish CICYT (BQU2001-3173-C02-01 and CTQ2004-03735/BQU). M.G.-A. wishes to thank Fundación Ana y José Royo from Valencia (Spain) for a postdoctoral fellowship. J.M.M.-B. and S.G.-G. are grateful for financial support from CICYT (BQU2003-0593).

**Supporting Information Available:** CIF file for the structure of the compound. This material is available free of charge via the Internet at <http://pubs.acs.org>.

IC050110C